



A Novel Approach for Measurement of Peak Expiratory Velocity

C. C. Wu[†] and F. M. Yu

Department of Aeronautics and Astronautics, National Cheng Kung University, Tainan 701, Taiwan ROC

[†]Corresponding Author Email: p48981219@mail.ncku.edu.tw

(Received August 19, 2015; accepted June 11, 2016)

ABSTRACT

It is well known that behind the orifice in a pipe, flow velocity increases and pressure decreases simultaneously. The generated sound appears that is caused by the pressure fluctuations that occur as the flow passes through the orifice. Then the flow velocity is averaged over a pipe cross-section and is considered as a constant, it can be seen that the amplitude of sound increases with increases in the expiratory velocity. An experimental study of the quantitative analysis of sound pressure level correlated with expiratory velocity in a pipe was conducted using an apparatus that includes an air pump in conjunction with a pipe, a microphone, and an orifice plate, among other instruments. The regression and analysis of the results shows that the pressure fluctuation of sound spectra can be correlated to the expiratory velocity of a pipe. The experiment is conducted under conditions where the air passing through the orifice has an averaged expiratory velocity ranging from 0.88 m/sec to 1.35 m/sec, an inlet temperature of 298.15 K, and where the outlet pressure is that of the atmosphere. In this experiment, the Mach number is very low, and the compressibility effects can be ignored. The obstacle orifice plate was placed in the center of the pipe, and a microphone was mounted flush downstream to acquire the sound pressure data on the pipe wall. The measured results show that the approach for measuring the expiratory velocity using a microphone can be justified, and there exists a good correlation between the Power Spectral Density (PSD) of sound pressure fluctuation and the peak expiratory velocity.

Keywords: Peak expiratory velocity; Wall-pressure spectra; pipe flow; PSD.

NOMENCLATURE

A	cross area	P_n	current pressure
A_1	area of the pipe	P^2	non-dimensional power spectrum
A_2	area of the stenosis	Q	volume flow rate
D	vessel diameter; pipe diameter	U	mean velocity in the arterial
d	stenosis diameter; orifice diameter	u_i	stream wise velocity
f	frequency	u_j	wall normal velocity
P_{tm}	mural pressure	\bar{u}	time averaged velocity component
P_{ao}	outside pressure	x_i	stream wise direction
P_A	internal pressure	x_j	wall normal direction
P_{pl}	airway pressure	ρ	fluid density
P_c	correction pressure	θ	normalized intensity
p'	pressure fluctuations	α	constant
Δp	differential pressure		

1. INTRODUCTION

Various devices, which include orifice gauges, Venturi pipe, ultrasound flow meters, Laser Doppler Anemometry, and so on, have been developed for determining the velocity of a flowing gas. They operate according to many different flow theories.

An innovative concept for noninvasive measurement of peak expiratory velocity that can offer small losses in flow pressure as well as low device costs was investigated in this study. The maximum expiratory volume depicts an important index for justifying human lung function, which represents the physiological relationship between expiratory

response and lung function. The measurement of air expiratory volume depends on its velocity, and a velocity meter can be used to assess this relationship to measurements of maximum expiration velocity. An innovative velocity meter device offers a simple method for expiratory velocity measurement with proper accuracy.

Farabee *et al.* (1986) investigated wall pressure fluctuations and concluded that spectral contributions at high frequencies were owed to turbulent velocity fluctuations on the wall region of the boundary layer. The contributions at low frequencies were the result of turbulent velocity fluctuations across the entire boundary layer. Rosser *et al.* (2014) studied a flow being sucked through an orifice plate and forming a jet downstream of the plate. The results showed that in addition to the noise associated with the acoustic response of the jet, a tone was produced by the interaction of the jet with the recirculation region behind the orifice plate. This acoustic tone is produced by turbulent patches, which is a result of convection from the recirculation region impinging on the jet with a characteristic passing frequency. The Strouhal number, fd/U , of the tone increases with orifice diameter. For a small orifice diameter, the Strouhal number of the tone is insensitive to jet velocity. However, for a large orifice diameter, the Strouhal number of the tone decreases with increasing jet velocity. It was found that this tone can be suppressed by using an appropriate insert downstream of the orifice plate. He observed that the tonal behavior from the orifice plate is independent of the thickness of the orifice plate. Gorin (2007) studied the near-wall behavior and heat and mass transfer in the turbulent separated flows. Separation of turbulent boundary layer is reported in experimental studies to be unsteady phenomenon consisting of local events of unsteady separations which occurs chaotically in the vicinity of the mean flow separation line. The generated local large-scale wall pressure gradient equaled to the sum of mean pressure gradient due to the variation of the free-stream velocity and the large scale fluctuating pressure gradient induced by the large-scale vortices of separated shear layer. Geropp *et al.* (2001) used a Prandtl sensor to perform flow rate measurements in turbulent pipe flows with minimal loss of pressure using a defect-law, which is a simple and very accurate measurement technique to determine volumetric or mass flow rate. It is based on a fully-developed turbulent pipe flow, which is an analytical universal velocity-profile over an entire pipe section with a single point measurement. In combination with an optimized straightener, this technique has shown minimal pressure loss at a moderate cost as compared to Laser-Doppler Anemometer measurements. Hasan *et al.* (2008) studied the sinusoidal fluctuated pulsatile laminar flow through stenotic artery using a numerical simulation. They found that the dynamic nature of pulsating flow disturbs the radial velocity distribution and thus generates recirculation zone in the post-stenotic region. The flow disturbances become more severe for higher stenosis size. Peak wall shear stress and wall vorticity appear to intensify at the throat of the stenosis. It is also observed that the peak wall

vorticity seems to increase with the increase of stenosis size and Reynolds number.

This study is based on the relation of sound pressure fluctuation to the peak expiratory velocity in order to provide a novel approach to fluid velocity meter measurement that can accurately measure peak expiratory velocity using a simple device. A simple apparatus was set up to demonstrate the functional relationship between unsteady flow pipe pressure spectra and velocity fluctuations. The effectiveness of this piping device is assessed by comparing the spectral data from a series of experimental measurements.

2. THEORY ANALYSIS ON A RESPIRATION SYSTEM

2.1 Bernoulli Effect

Bates (2009) described a clinical assessment of lung function that is most commonly used based on expiratory flow limitations in which the magnitude of the flow leaving the lung does not increase indefinitely with the expiratory pressure generated by the respiratory muscles. Fig. 1 shows a model of the respiratory system in which flow is constrained by resistance in the airway. Depending on the viscosity, air density and jet velocity variation, the air stream transitions from laminar to turbulent. With air flowing at a rate along a conduit of a constant cross-section area, the measured pressure at any point on the conduit wall is less than the inflow pressure driving the flow. The pressure gradient in a conduit with a varying cross-section is proportional to the axial flow velocity, and there is a linear relationship between its mural pressure (P_{tm}) and cross area (A). If the slope of the relationship is dP_{tm}/dA , then the value for the maximal air flowing at a rate as:

$$Q_{max} = A \sqrt{\frac{A}{\rho} \frac{dP_{tm}}{dA}} \quad (1)$$

Assuming the cross area and air density in the same conduit is constant.

$$Q_{max} \propto \left(\frac{dP_{tm}}{dA} \right) \quad (2)$$

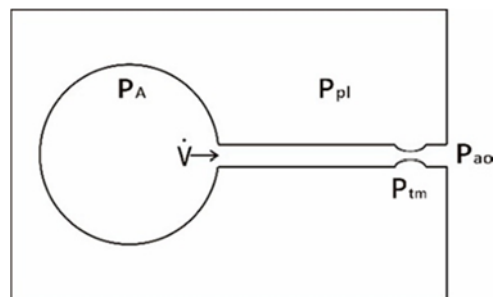


Fig. 1. Stylized model of the respiratory system.

2.2 Poisson Equation for a Turbulent Shear Flow

Capone *et al.* (1993) described the turbulent pressure

fluctuations on the experimental measurements of a turbulent boundary layer using its wall pressure spectra. With the flow transitions from laminar to turbulent, velocity fluctuations within the boundary layer became pronounced and ranged up to 50% of the mean flow velocity. As a result of the dramatic velocity fluctuations within the turbulent boundary layer, the pressure at a given point in the flow also fluctuated with time. When the flow is assumed to be homogeneous in the plane of the wall, a two-dimensional flow can be considered. To determine the wall pressure spectrum due to the turbulent boundary layer, the relationship between the fluctuating velocities and pressure must be defined, which can be shown as:

$$\frac{\partial^2 p'}{\partial x_i^2} = -\rho \left\{ 2 \frac{\partial u_i}{\partial x_j} \frac{\partial u_j'}{\partial x_i} - \frac{\partial^2}{\partial x_i \partial x_j} (u_i' u_j' - \bar{u}_i' \bar{u}_j') \right\} \quad (3)$$

The first term on the right-hand side of equation represents the interaction of the mean shear in the flow with the turbulence. The second term on the right-hand side of the equation represents the turbulence-turbulence interaction. This equation shows that the fluctuating velocities within the turbulent boundary layer are the source of the pressure fluctuations generated by the boundary layer.

2.3 Wall Pressure Spectrum in Turbulent Pipe Flows

Lees *et al.* (1970) described a noninvasive diagnostic method for studying arterial disease. The quantitative analysis of sounds produced by blood flow was used to investigate the local fluid motion in an artery narrowed by atherosclerosis. Flow through an orifice often produces a free jet even at low Reynolds numbers. This jet of fluid becomes unstable and converts a portion of its kinetic energy into turbulent fluctuations. The turbulence produces pressure fluctuations at the vessel wall that can be detected as arterial sounds. Well-developed turbulence is characterized by a spectrum in which the intensity decreases rapidly with increasing frequency. The non-dimensional power spectrum is a function of the non-dimensional frequency. Fig. 2 presents the production of sound by post stenosis turbulence.

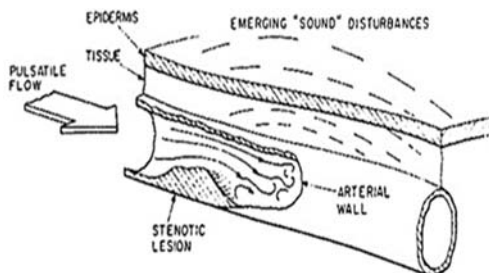


Fig. 2. Schematic representation of a stenosis peripheral artery showing the production of sound by post stenosis turbulence.

The total normalized intensity is the integral of the power spectrum, and the mean velocity proximal to the stenosis and the velocity at the stenosis can be characterized. Neglecting the Reynolds number effects, the following was observed:

$$P^2 \propto \frac{v^2}{\alpha^4 \rho^2 D U^3} \left(\frac{d}{D}\right)^8 \quad (4)$$

The total normalized intensity, θ , had a relationship with the power spectrum.

$$\theta \propto P^2 \propto \frac{\left(\frac{d}{D}\right)^8}{\Delta f U^3} \quad (5)$$

2.4 Relationship between the Radiated Sound Pressure Spectra and the Rate of Flow

Rahman *et al.* (2009) studied the effects of beta ratio and Reynold's number on the coefficient of orifice meter discharge, and the results show that as the fluid approached the orifice, the pressure increased slightly and then dropped suddenly as the flow moved behind the orifice. The pressure variation is a result of the increasing of velocity as the air passed through the reduced area of the orifice. The total pressure loss was not recovered because of friction and turbulence losses in the stream. The pressure drop across the orifice increased with the rate of increase in the flow. Zhang *et al.* (2004) studied sound generation using steady flow through glottis-shaped orifices, and they found that the radiated sound pressure spectra in air varied for different values of orifice pressure drop. The spectra level increased with the drop in pressure. It was found that the radiated sound pressure spectra of the air passing through an orifice plate increases when the expiratory velocity at the inlet of the straight pipe plate increases.

3. EXPERIMENT APPARATUS

3.1 Fluid Velocity Meter Design

Farber *et al.* (1963) found that when the blood is flowing in the arteries, if the transverse motion of the wall is impeded, it follows that the murmur is attenuated at the location of the stenosis as recorded by a microphone. According to the notion that designing a simple and fast measurement device that can accurately measure peak expiratory velocity, a simple air pump was included in the apparatus used in this study with various blockage blocks and a microphone device on the pipe wall is used to acquire the flow data and to calculate the peak expiratory velocity. The measured data was stored through analogy-to-digital converter (A/D) to a computer for further analysis. Finally, this system was measured in an indoor environment.

The experimental apparatus used in this study consists of a simple air pump as the source of steady air, and an orifice plate with three beta ratios is used. A microphone on the pipe wall was used to acquire the flow signals. A digital camera was used to detect the piston moving displacement of the air pump, and then the air velocity was calculated. The air pump

outlet was attached to a circular pipe, and 35 mm behind the junction, a bundle of honeycomb-structured tubes was mounted to straighten the flow. The pipe was 18 mm in diameter, 273 mm in length, and had a 1.5 mm wall thickness, with a length-diameter ratio of 15.2. A bundle of honeycomb-structured tubes 4 mm in diameter, 28.5 mm in length, and 0.1 mm wall thickness, with a length-diameter ratio 7.13 was used to straighten the stream from the piston tube. This honeycomb bundle shielding area made up 8.4% of the testing pipe cross sectional area. An orifice plate with a 9.8 mm opening was placed in the center of the pipe. The orifice plate was 1.5 mm thick, as shown in Fig. 3. The orifice plate was installed 100 mm behind the junction in the pipe. The microphone was installed on the pipe wall for the measurement of the sound pressure. It was connected directly to an A/D converter, and the data was transferred to a computer for storage and signal analysis.

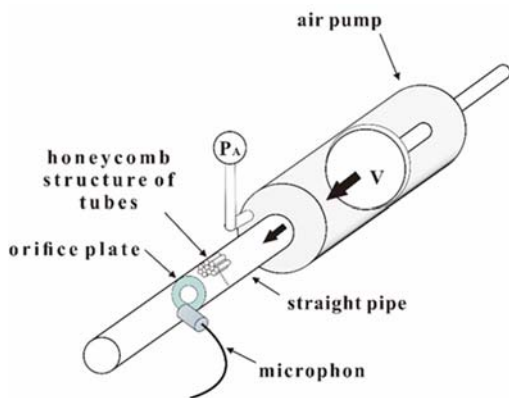


Fig. 3. Simple air pump, ventilation pipe and microphone.

3.2 Signal Acquisition System

The USB-6341 A/D converter device from the National Instrument Company was chosen for data acquisition. It has 8 analog inputs, 2 analog outputs, 24 ports for digital input or output, and it has a maximum sample rate of 500K Hz. In addition to the ports in the USB-6341 for data acquisition, there is also 1 port for powering an external device (+5.0V). The microphone was connected to the analog input of the USB-6341 with a 16 bit resolution A/D converter, and the data was acquired with a personal computer for further processing. The sampling accuracy of the USB-6341 is at 2-16 or 0.0001525, and all measurements had an accuracy of 0.001. LabVIEW software was used to develop the data acquisition program to read the converted A/D signal and perform the signal analysis.

3.3 Microphone Calibration

The microphone is the device used to measure the sound field. It responds to sound pressure and transforms it into an electric signal that can be interpreted by the measurement instrument. A corrected high sensitivity 6.4 mm diameter condenser microphone with associated analogy

interfacing circuitry was used to acquire the sound pressure signals in this study. As the sound pressure signals are transferred to the computer, it can resolve the existence of a peak pressure value, and it reflects the intensity of the flow-field fluctuation. Sound pressure is typically referred to as the effective sound pressure, which is the root-mean-square (RMS) value of the instantaneous sound pressure taken at a specific point over a period of time. In order to take scientific measurements with a microphone, its precise sensitivity must be calibrated. In this study, this calibration was done using the Brüel & Kjær Type 3541 sound calibrator as shown in Fig. 4.



Fig. 4. Brüel and Kjær Type 3541 sound calibrator.

Type 3541 calibrators are highly dependent on ambient pressure and are generally only made to reproduce low frequencies, typically 250 Hz, which are very precise and have good stability over time. When a microphone is positioned in the Type 3541 calibrator, the simulated sound wave can be used for calibrating the sensitivity of the measuring instrument to sound pressure which produces a sound pressure level of 117.8 dB re 20μPa at each channel of the intensity coupler. Sound pressure level, which is often abbreviated as SPL, in decibels, can then be obtained using the following formula.

$$SPL = 20 \log_{10} \frac{P_{rms}}{P_{ref}} \quad (6)$$

The microphone's sensitivity and frequency response are affected by variations in the ambient pressure. This is due to changes in the compliance of air volume inside the microphone, so that the P_{rms} values varied with varying of the ambient pressure. The microphone can measure the sound signals, which is due to the sound pressure variations acting on a microphone diaphragm behind the air volume. It has been observed that the measured sound pressure using same microphone at different ambient atmospheric pressure the measurement results cannot compared to each other. Since their compliance of the air volume inside microphone is different under different ambient atmospheric pressure. Before the proper calibration, the ambient pressure was measured and the corrections terms for the calibration levels were calculated.

$$P_c = (P_n - 1013) \times 8.4 \times 10^{-3} \quad (7)$$

Then, the corrected values of SPL were inter-

compared on different days for science and engineering applications. For example, the sound pressure fluctuations on the artery using a microphone can use to determine the artery stenosis, if the SPL is present. Therefore, it is necessary to calibrate measurement microphones every day to obtain the corrected $SPL_{corrected}$. According to the instruction manual for the Type 3541 calibrator, ambient temperature has almost no influence on the microphone.

$$SPL_{corrected} = P_c + 20 \log_{10} \frac{P_{rms}}{P_{ref}} \quad (8)$$

4. EXPERIMENTAL RESULTS AND DISCUSSION

4.1 Wall Pressure Spectrum in Turbulent Pipe Flows

On the ventilation pipe, the measured air signal from the microphone was output as a set of voltage signals. The sampling frequency was set at 2500 Hz and 5,000 samples were collected by sweeping the signal with a narrow-band frequency filter. The filter specified in this program was a Butterworth filter with pass-band frequencies for which cut off is set internally by National Instruments to correlate with the sampling rate. The air pump pushed a fixed volume of air into the ventilation pipe, and the microphone sound pressure data and output signals were measured as shown in Fig. 5. The relationship between sound frequency and the transmission velocity was studied with this microphone. Since this jet flow is not steady, the frequency of maximum oscillation power cannot accurately be recovered from the microphone signal. With fluctuating pressure over time during the testing process, the fluid characteristics could not be recognized easily. However, the sound was characterized by the PSD of the signal, with sound intensity mapping as shown in Fig. 6. It was found that the greatest signal intensity was distributed between 140 and 160 Hz within the frequency range.

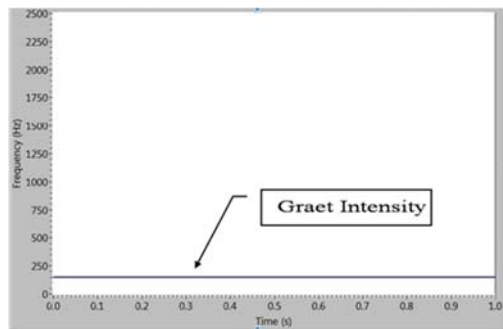


Fig. 5. Microphone output signals.

The measured sound was the result of a transverse pressure fluctuation on the pipe wall. The dominant contributions from the unsteady flow appear in the low frequency portion of the spectra of the measured sound. Fig. 7 shows the PSD plot of the measured sound. The PSD is proportional to the intensity of the air flow passing through an orifice plate, and the

unsteady flow intensity of expiratory air depended on the inlet air flow velocity of the pipe. As stated before, the PSD of the measured sound was observed to increase with the expiratory velocity of the inlet pipe within a frequency range from 140 to 160 Hz. As a piston type pump is pushed down, the air is forced to blow through the orifice plate. There are eight force levels to push the air pump, and there are eight different air inlet velocities to be examined. At each force level, the microphone signals were measured for five seconds continuously at each testing. The digital PSD data for the measured sound between 140 and 160 Hz was put in column text type for the subsequent statistics and other data analysis.

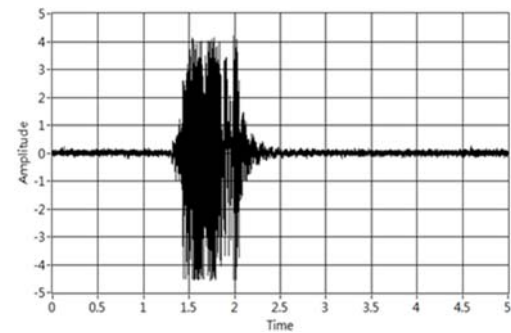


Fig. 6. Graphic illustration of signal intensity.

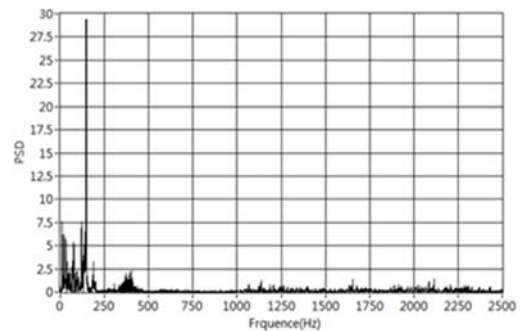


Fig. 7. The PSD of the measured sound.

4.2 Effect of Orifice Diameter

Three blockages in the orifice plate with opening diameters of 5.8, 9.8 and 13.7 were tested. Each of the orifice plates was tested at a different air inlet velocity to measure the output PSD of the sound and to obtain the trend curve of the sound using regression analysis. Eight levels of the driving forces used in this study are shown as Table 1, and the other parameters for the testing orifice plates are presented in Table 2.

Table 1 Results of the testing of eight force levels

Force Level (kg)	0.4	0.5	0.6	0.7	0.8	0.9	1	1.05
Expiratory Velocity (m/s)	0.88	1.05	1.10	1.18	1.21	1.23	1.26	1.35

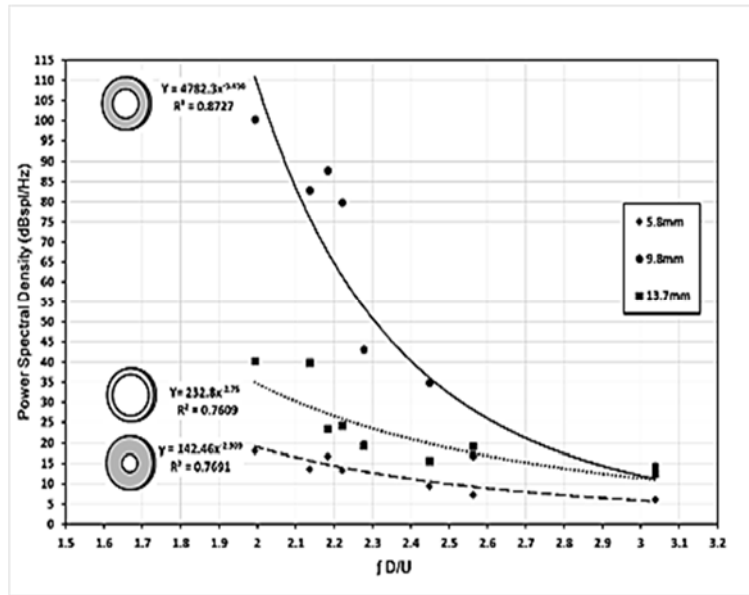


Fig. 8. PSD of the different testing models.

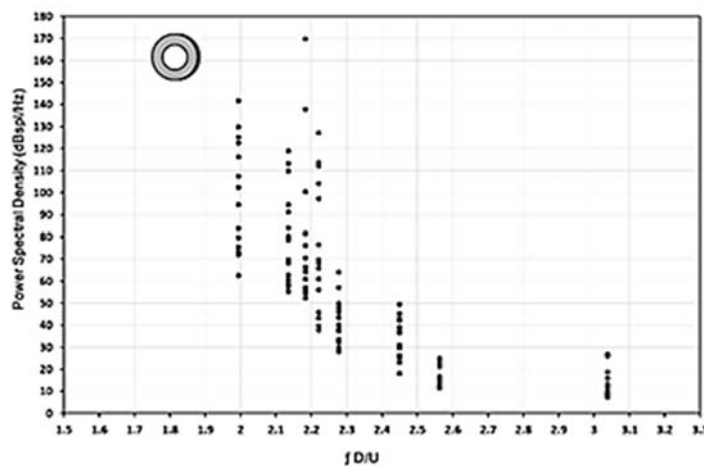





Fig. 9. PSD for Model 2.

Table 2 Parameters for each opening in the orifice plate

Openings			
Testing Model	1	2	3
Diameter (mm)	5.8	9.8	13.7
Vent area Rate (%)	10.38	29.64	57.93
Beta Ratio	0.32	0.54	0.76

The discharge velocity of the air pump was obtained accordingly from the displacement of the piston with time, and the measured sound was recorded. This

process was repeated about 15 times for each opening in the orifice plate at every force level to acquire the amount of data required for plotting the trend curve of the ventilation pipe.

The measured results are shown in Fig. 8, which shows the trend curve of each model. On the sound spectrum, it was found that Model 2 was much higher than the other models in lower reduced frequency. Because of the use of industrial experimental data, it can be found that the concentric orifice plate of minimum uncertainty occurs for a beta ratio of between 0.20 and 0.60 for gases. The best results occur at a beta ratio between the values of 0.4 and 0.6 on the AGA report No.3-Third Edition Part 1 (1990). It can be found that the orifice meter with a beta ratio of nearly 0.55 can be used for effective pipe flow measurement, in which the percent of uncertainty is at a minimum, and this

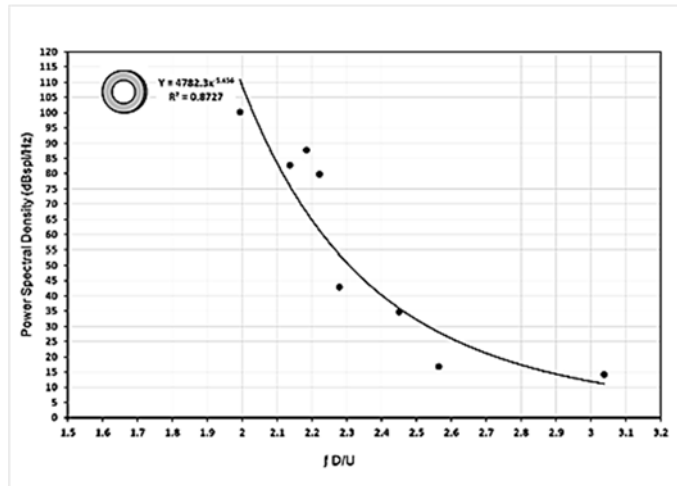


Fig. 10. RMS value of the PSD for Model 2.

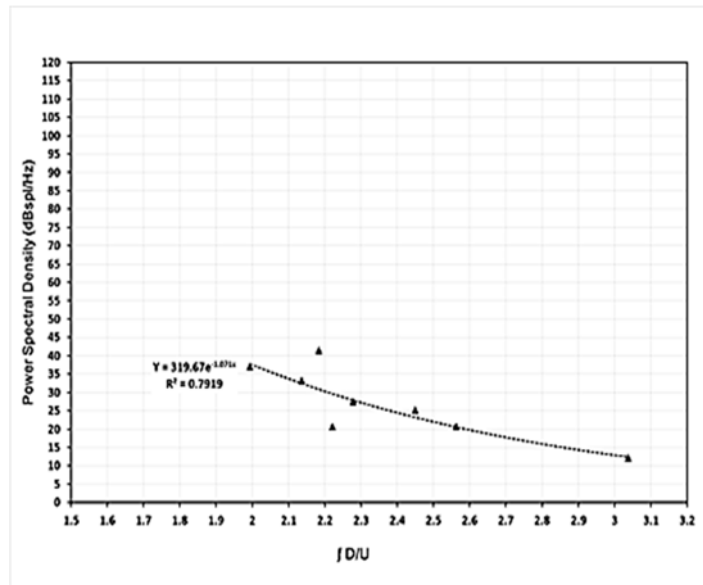


Fig. 11. RMS value of the PSD for Model 4.

study suggests an orifice plate with a bore diameter of less than 11.4 mm for the current ventilation pipe. From this experimental data, it can be found that the PSD of the beta ratio of 0.54 is largest at the lowest reduced frequency, fD/U , and beta ratios of 0.32 and 0.76 have a greater percent of uncertainty, which influences the PSD of the measured sound. Therefore, the beta ratio of 0.54 is better than the others as shown by the increase in the inlet expiratory velocity with the decrease in the PSD (see Fig. 8).

4.3 Signal Processing

The PSDs of Model 2 at various velocities are shown in Fig. 9. It can be seen that the measured PSD has a wide range of distribution for each reduced frequency.

From the Poisson Equation for a unsteady shear flow, Eq. (3) shows that the source of the pressure fluctuations consists of contributions from the mean-

shear-turbulence interaction and the turbulence-turbulence interaction. Only the stream-wise component of the mean velocity is significant in the flow of the orifice plate, and the turbulence-turbulence term is second order. Therefore, the turbulence-turbulence terms can be neglected. Thus, the fluctuating pressure equation can be reduced to:

$$\frac{\partial^2 p'}{\partial x_i^2} = -2\rho \frac{\partial u_i}{\partial x_j} \frac{\partial u_j'}{\partial x_i} \quad (9)$$

As air flow passes through the orifice plate, it forms a jet surrounded by an annular recirculation region which transmits small eddies and produces broadband noise. This noise is produced by the jet inside the orifice plate after it transitions to unsteady flow. When the velocity increases, the distribution of the noise becomes wider and influences data distribution. The root mean square (RMS) method is commonly used to characterize sound waves because it is directly related to the energy carried by the

sound waves. The following results show that the RMS value for the PSD under various deriving forces using an air pump is significant. The RMS value of the PSD for Model 2 is shown on Fig. 10. The RMS value of the PSD decreases when the reduced frequency increases. The correlation indicates a stronger relationship between them and on the beta ratio of 0.54, the R^2 value is 0.8727. The curve fit can be shown as:

$$Y = 4782.3x^{-5.456} \quad (10)$$

For a measured PSD equal to 50, then using the formula $Y=4782.3x^{-5.456}$ can solve the x value of 2.3068. Therefore, the peak expiratory velocity can be calculated, which is approximately 1.1705 m/s by the reduced frequency. As a result, it can be a useful tool on measuring the expiratory velocity of a pipe with a known inner diameter.

In Fig. 10 above, the RMS value of the PSD is proportional to the air inlet velocity, and Eq. (9) shows that the air flow passing through the orifice plate has two disturbing effects: contraction of the flow after a sudden change in the cross-section and friction at the walls. To find out the role of the sudden change in the cross-section and friction at the walls in this case, a straight ventilation pipe 18 mm inner diameter without any blockage is tested as Model 4. The test results are shown as Fig. 11, and it can be seen that the measured RMS for the PSD of sound in this pipe is mainly introduced by noise due to friction on the pipe wall because the RMS value of the PSD slightly decreases as the reduced frequency increases. The gradient is smaller compared to the results from Model 2. The curve fit equation can be expressed as:

$$Y = 319.67e^{-1.967x} \quad (11)$$

When comparing Fig. 10 and Fig. 11, under higher reduced frequency, which means a flow with lower expiratory velocity, the measured RMS values of the PSD are very close for each test case. This indicates at a lower expiratory velocity, the flow passing through a blockage in the ventilation pipe cannot generate a strong sound. It can be observed that the measured signal from the microphone installed on the ventilation pipe with blockage was not obvious. As the value of fd/U decreases, which indicates that the expiratory velocity increases, the measured RMS of the PSD increases as well. By Fig. 10 and Fig. 11, the effect of friction at the walls could vary with the inlet expiration velocity, and by comparison, the effect of a contraction of the flow after a sudden change in the cross-section is smaller. It can be seen that the measured RMS values of the PSD are mainly made by the area of contraction at a high expiratory velocity. Further, the friction at the wall spectrum is small, which can be neglected.

The sound in the pipe with obstacle is a result of the resulting flow disturbance due to large scale coherent vortex structure and turbulence, which is expected to exhibit important characteristics on the scattering of sound waves, e.g. the frequency of a sound, sound pressure distribution, PSD of sound pressure fluctuation and so on. This study is conducted to analyze the characteristic sound signals and to reveal

the relationship between the peak expiratory velocity and the PSD of sound pressure fluctuation behind an orifice with different Strouhal numbers. Assuming that changes in air density and viscosity are negligible, the air velocity is directly related to the pressure fluctuation, which means that the expiratory velocity varies with variations in pressure. In this study, the correlation curve exhibited a good trend. The experimental results show a good correlation between the PSD of sound pressure fluctuations and the peak expiratory velocity. It suggested that a microphone can be used to measure the sound pressure fluctuation of downstream of the orifice and it can be correlated to the peak expiratory velocity. Furthermore, if the measured flow has known thermodynamic properties, the volume flow rate per unit area can be obtained from this result. This information can offer a wide range of application possibilities for various peak volume flow rate measurement applications.

5. CONCLUSION

Experiments were performed to study sound radiation from air flow passing through various blockages. Four testing models were studied at different air inlet velocities, and a production of sound by post blockage characteristic were found. To characterize the sound wave, the RMS method was used to perform signal processing and to create a trend curve based on the experimental results. Comparing and contrasting Fig. 10 and Fig. 11, a significant difference can be seen in the sound field of the ventilation pipe with and without a blockage observed at a higher expiratory velocity. In this study, the trend curve was correctly identified and was in concurrence with previous studies on ventilation pipes with blockages. The testing results suggested that a novel approach to an expiration flow meter can be proposed, which is a partially blocked ventilation pipe of a finite diameter with a microphone downstream of the blockage. The measured sound RMS of the PSD was found to be related to the peak velocity of the expiration flow, and the effectiveness of the proposed method was proven.

REFERENCES

- (1990). AGA 3.1: Orifice metering of natural gas and other related hydrocarbon fluids: Part 1, American Gas Association, Washington, 6-37.
- Bates, H. T. Jason (2009). *Lung mechanics: an inverse modeling approach*, Cambridge University Press, New York 97-107.
- Capone, D. E. and G. C. Lauchle (1993). Calculation of turbulent boundary layer wall pressure spectra. *The Pennsylvania State University Applied Research Laboratory Technical Report* 93-10 4-11.
- Farabee, T. M. (1986). *An experiment investigation of wall pressure fluctuation beneath non-equilibrium turbulent flows*. Ph. D. Thesis, Naval Ship Research and Development Center,

- Bethesda, MD.
- Farber, J. J., and J. H. Purvis (1963). Conduction of cardiovascular sound along arteries. *Circulation Research* 12, 308-316.
- Geropp, D. and H. J. Odenthal (2001). Flow rate measurements in turbulent pipe flows with minimal loss of pressure using a defect-law. *Flow Measurement and Instrumentation* 12(1), 1-7.
- Gorin, A. (2007). Turbulent separated flow: near-wall behavior and heat and mass transfer. *Journal of Applied Fluid Mechanics* 1(1), 71-77.
- Hasan, A. B. M. T. and D. K. Das (2008). Numerical of sinusoid fluctuated pulsatile laminal flow through stenotic artery. *Journal of Applied Fluid Mechanics* 1(2), 25-35.
- Lees, R. S. and C. Forbes Dewey Jr (1970). Phono-angiography: a new noninvasive diagnostic method for studying arterial disease. In *Proceeding of the National Academy of Sciences* 67(2) 935-942.
- Rahman, M. M., R. Biswas and W. I. Mahfuz (2009). Effects of beta ratio and Reynold's number on coefficient of discharge of orifice meter. *Journal of Agriculture and Rural Development* 7(1 and 2), 151-156.
- Rosser, C. J. and A. Agarwal (2014). The acoustic of suction. *The 7th Conference of Forum Acusticum 2014 Krakow at the AGH University of Science and Technology*, Poland.
- Zhang, Z., L. Mongeau S. H. Frankel and S. Thomson (2004). Sound generation by steady flow through glottis-shaped orifices. *Acoustical Society of America* 116(3), 1720-1728